The 19th Conference of Mechanical Engineering Network of Thailand
19-21 October 2005, Phuket, Thailand

Modelling of Powders with Internal Pores in Cold Compaction

Somboon Otarawanna [1], Wiwat Tanwongwan [1], Anchalee Manonukul [1]* and Julaluk Carmai [2]

[1] National Metal and Materials Technology Center, Klong Luang, Pathumthani 12120
[2] Department of Production Engineering, Faculty of Engineering, King Mongkut's Institute of Technology North Bangkok, Bangsue, Bangkok 10800
*Corresponding author (E-mail: anchalm@mtec.or.th)

Abstract

Powders used in the powder compaction could be solid or sponge powders depending on the powder fabrication techniques. This paper is the first attempt to theoretically investigate sponge powder compactions with different levels of initial relative density. Cold compactions of regular-density, high-density sponge powders and solid powders have been studied using the 'explicit particle modelling' approach. The spongy morphology in each sponge powder is modelled by the porous constitutive model and 'explicit modelling of internal pores' approach for comparison purpose. The results suggest that the present of internal pore has an effect on the macroscopic stress response. The high-density sponge powder with a large number of very small isolated internal pores is apparently stiffer than the others. The regular-density sponge powder with high internal connected porosity requires lower macroscopic stress to deform than the others at the same relative density excluding internal pores. Where both internal and external pores are present at the initial stage of the compaction, the deformation is preferential towards the external pores.

Keywords: Powder compaction; Constitutive material model; Sponge powder; Internal pore

1. Introduction

Different powder fabrications can lead to powders with different characteristics. The fabrication of powders involves the application of energy to materials to create new surface area. Selection of a certain fabrication technique depends on understanding of a process, its economics, the resulting powder characteristics, and how those characteristics satisfy the desirable application. Two different popular fabrication techniques for metallic powders are oxide reduction and atomisation. Oxide reduction is a classical powder fabrication technique which can be achieved by thermochemical reactions of metallic oxide involving reducing gases such as hydrogen or carbon monoxide. Atomisation is an advanced powder fabrication technique which involves the formation of powder from molten metal using a spray of droplets. Typically, powders fabricated by oxide reduction are spongy, while powders fabricated by atomisation are solid as shown in figures 1(a) and (b) respectively. Sponge powders are commonly used for the production of low to medium density ferrous powder metallurgy parts, approximately 5.5 g/cm^3 to 7.0 g/cm^3 [1]. On the other hand, water atomised powders are commonly used for the production of high density alloyed parts. For powder compaction modelling, this can be carried out using the approach of 'explicit particle modelling' which models individual powder explicitly. From the literature [2-6], the explicit particle modelling has only been employed to model powders containing no internal pores regardless that the powders are solid or spongy.

This work is the first attempt to truly represent spongy morphology. The compactions of solid powders and sponge powders with regular and high initial relative densities are modelled to investigate the deformation behaviour of sponge powders comparing to that of solid powders. (The relative density is defined as the ratio of the bulk density of porous media to its theoretical density.) Behaviour of each sponge powder is modelled using the constitutive material models for porous material. The modified Drucker-Prager Cap model and the porous metal plasticity (Gurson) model are employed to model sponge powders in the case of regular and high initial relative densities respectively. In addition, the compaction of high-density sponge powders is also performed using the approach of 'explicit modelling of internal pores' to compare the results with those of the constitutive modelling

2. Numerical Analysis Procedures

The explicit particle modelling approach is used in this investigation to study the deformation of individual powder. The problem is solved numerically using a finite element analysis tool. In the past, only finite element modelling using two-dimensional plane strain elements has been reported in the literature [2-6]. The reasons for only using the two-dimensional element could be the limitation of computational power and the robustness of the contact algorithm in the finite element software. Comparison of finite element analysis using the two-dimensional plane strain, two-dimensional generalised plane strain and three-dimensional solid elements for modelling powder compaction was carried out and reported elsewhere [7]. It was found that the two-dimensional plane strain solid element is suitable for further investigation considering the accuracy and the effort required. Therefore, the two-dimensional plane

strain solid element has been employed in this investigation.

To solely investigate the effects of the spongy morphology within the powder, mono-size circular particles packed together with hexagonal closed-packed (HCP) arrangement are considered here. The well-known 'repeated representative unit cell' concept is applied since the powders are uniformly arranged. The HCP arrangement of mono-size circular particles and its representative unit cell with symmetry conditions imposed are illustrated in figures 2(a) and (b) respectively.

The internal pores within each powder can be modelled by two approaches: (1) implementing the constitutive material model for porous material to model each sponge powder with internal pores and (2) creating arbitrary small holes within each powder to represent the internal pores, so-called explicit modelling of internal pores approach. Figures 3(a) and (b) show the finite element models representing the uniaxial compactions of HCP-arranged mono-size circular powders by these two approaches respectively. Only a quarter of the unit cell is modelled due to symmetry. The top and right boundaries of the unit cell are constrained to remain straight for compatibility. The bottom and left boundaries are the symmetry boundaries. The contacts between each powder, so-called 'interparticle contact', are treated as frictionless contact pairs to solely investigate the effects of internal pores on the deformation. In the cases of solid powders and explicit modelling of internal pores, the property of each powder is defined by the linear elastic Hooke's law and the Mises platicity model with linear hardening modulus. On the other hand, the constitutive porous material models are represented the behaviour of sponge powders in other cases described in the next section.

3. Constitutive Material Modelling of Internal Pores

There are two main approaches for constitutive model development for porous material: micromechanical and phenomenological models. The micromechanical model for the low relative density range has been developed by assuming that the porous material contains spherical powders and these powders are joined by isolated contacts which form connecting voids. When the relative density of porous material is higher, the voids between powder interactions become isolated. The micromechanical model for high relative density range, therefore, is based on the assumption that the porous material consists of a matrix containing isolated spherical voids. As for the phenomenological model, it assumes a complex yield surface with many material parameters to capture the complicated response of porous material.

In a general-purpose finite element software [8], there are two available constitutive models that can be applied to model the powder compaction process: the porous metal plasticity (Gurson) model and the modified Drucker-Prager Cap model. The porous metal plasticity model is a micromechanical one suitable for high relative density range whilst the modified Drucker-Prager Cap model is a phenomenological one able to use for all ranges of relative density. The yield surfaces in the meridional (pressure stress p - deviatoric stress t) plane of these two models are shown in figures 4(a) and (b) respectively.

To calculate the apparent density of each sponge powder, one of the most popular sponge iron powder, Ancor® MH-100 of Hoeganaes Corp. [9], is considered here. The density is 2.55 g/cm^3 , which is equivalent to the relative density of approximately 0.4 in two-dimensional (shown in Appendix A). Hence, the apparent density of each sponge powder will be approximately 0.44 (shown in Appendix B). The simulation with the relative density value of 0.44 for porous media can only be performed by the modified Drucker-Prager Cap model because the lowest possible relative density of the porous metal plasticity model is 0.9. With this regard, the sponge powder with apparent relative density of each powder higher than 0.44 is also selected to study. Consequently, the simulations of sponge powder compaction with regular initial relative density of 0.4 (0.44 for each powder) and a high initial relative density of 0.82 (0.9 for each powder) are represented by the modified Drucker-Prager Cap and the porous metal plasticity models respectively.

4. Explicit Modelling of Internal Pores

For the explicit modelling of internal pores approach, each sponge powder can be modelled by the solid section with arbitrary small holes representing the internal pores within each powder. However, this approach can only apply to the case of high-density powder because of the assumption of isolated internal pores [10]. In this work, twenty four circular internal pores are uniformly located within each powder. As the result, each quarter shown in figure 3(b) contains only six circular holes. Hence, each powder has the ratio of holes to powder area equal to 0.1.

In figure 3(b), the finite element model contains many contact pairs and involves large deformation of elements surrounded the internal holes. Consequently, the explicit finite element solver [11], which has more stable contact algorithm, is employed for retaining the solution accuracy. Generally, the compaction process can be assumed as a quasi-static problem. Therefore, the energy content checking should be performed after running the explicit solver to ensure the quasi-static assumption. The kinetic energy of the deforming material should not exceed 5% of its internal energy throughout the majority of the forming process [11].

5. Results and Discussion

The macroscopic stress, calculated from the compaction force divided by the compaction area, at each instant is recorded. Figure 5 shows the macroscopic stresses at different levels of relative density for all four cases: (1) regular-density sponge powder defined by the modified Drucker-Prager Cap model, (2) high-density sponge powder defined by the porous metal plasticity (Gurson) model, (3) high-density sponge powder using

explicit modelling of internal pores approach and (4) solid powder from atomisation. Although the high-density sponge powder defined by the porous metal plasticity model and the high-density sponge powder using explicit modelling of internal pores cases have the same initial relative density, the macroscopic stress responses are significantly different. The sponge powder defined by the porous metal plasticity model case requires higher macroscopic stress at the same relative density. The porous metal plasticity model is based on the distribution of small isolated spherical pores within each powder while the size of pore in the explicit modelling of internal pore is significantly larger. Deformation of larger pore is easier. Hence, the high-density porous metal plasticity model case is apparently stiffer. On the other hand, although the regular-density sponge powder defined by the modified Drucker-Prager Cap model, the high-density sponge powder using explicit modelling of internal pores approach and the solid powder cases have different initial relative densities, the corresponding macroscopic stress responses are very similar at high relative density.

When the relative density goes towards the value of unity (fully dense), the force required to cause further compaction is significantly larger. This is because the amount of space occupied by the internal pores is very small so the matrix material only has limited areas to flow and becomes effectively incompressible. Therefore, in the range of very high relative density (approximately more than 0.97), the macroscopic stresses of the sponge powder defined by the modified Drucker-Prager Cap model and the sponge powder using explicit modelling of internal pores approach cases become close to that of the solid powder. The case of high-density sponge powder with the porous metal plasticity model, however, gives the excessive higher values of macroscopic stress because of the limitation of its model when the relative density approaches to unity [6].

Figure 6 shows the macroscopic stresses at different levels of 'relative density excluding internal pores'. The relative density excluding internal pores is calculated by the same way as the regular relative density but the internal pores within each sponge powder are considered as solid. As the results, all porous cases have the same initial relative density excluding internal pores as the solid powders as shown in figure 6. At each level of relative density excluding internal pores, the solid powder gives the highest macroscopic stress and the regular-density sponge powder gives the lowest. The reason is that the regular-density sponge powders have the highest amount of space occupied by internal pores whilst the solid powders have none.

When the relative density excluding internal pores reaches the value of 1.0, the regular-density and high-density sponge powders can be pressed further because the internal pores still exist. Both cases give close values of macroscopic stress as the solid powder when the compact becomes fully dense. Nonetheless, the porous metal plasticity model still gives excessive high macroscopic stress because of the model limitation described above.

The deformation shapes of the sponge powder defined by the porous metal plasticity model and using explicit modelling of internal pores approach are showed in figures 7(a) and (b) respectively at different relative densities. Considering the external pores between contacted powders, the shapes of the pores are similar in both cases. Both cases have the same initial relative density of 0.82. At the initial stage for both cases, the sizes of external pores are the same. However, as deformation progresses, for the sponge powder defined by the porous metal plasticity model case, the size of external pores is smaller at the same level of relative density. This confirms the earlier discussion that this sponge powder is apparently stiffer than the sponge powder using explicit modelling of internal pores approach. In both cases, the external pores have become very small at the relative density of 0.97 and eventually will disappear. Further deformation can continue by reducing the size and the number of the internal pores. In the case of the sponge powder using explicit modelling of internal pores approach, although the initial shape of internal pores is circular, compaction loading causes the pore shape to deform and loose circularity. The shape of internal pores excluding the one closest to the centre of the powder becomes oval and inclined approximately 45° to the direction of applied load where the shear stress is maximum.

Figures 8 (a) and (b) show the decreasing rates of change of the volume fraction of internal or external pores with respect to the rates of change of the total volume fraction of pores for the sponge powder defined by the porous metal plasticity (Gurson) model and using explicit modelling of internal pores respectively. The rates of internal and external pores at any instant are always added up to unity. For both cases, when both internal and external pores are present, the deformation will tend towards reducing the size of the external pores. At low relative density, the size of the external pores is significantly larger than that of the internal pores and it is easier to reduce the size of the larger pores. As deformation continues, the external pores become smaller and more comparable to the internal pores, the rate of change of the external pore decreases while the rate of change of the internal pore increases. In the case of the sponge powder defined by the porous metal plasticity model, the initial rates of change for internal pores and external pores are zero and one respectively, while in the other case, the initial rates of change for internal and external pores are approximately 0.1 and 0.9. This is the result of the relative sizes of the internal and external pores. In the case of the sponge powder defined by the porous metal plasticity model, the relative sizes are significantly different. Hence, all initial loading is towards deforming to reduce the size of the larger external pores. In the case of the sponge powder using explicit modelling of internal pores, internal and external pore sizes are comparable since the internal pore size is defined explicitly which is subjected to the modelling

limitation. The initial loading is, thus, shared by the deformation of reducing external and internal pores. Nevertheless, the deformation is still preferential towards reducing the size of the external pores. This situation is inverted as the relative density becomes higher.

6. Conclusions

The theoretical study of sponge powder compactions with different levels of initial relative density has been carried out to investigate the effects of internal pores on the deformation behaviour. The results suggest that the present of internal pore has an effect on the macroscopic stress response. The high-density sponge powder with a large number of very small isolated internal pores is apparently stiffer than the others. At the same relative density excluding internal pores, the regular-density sponge powder with high internal porosity is easier to deform than the others. At the initial stage of the compaction where both internal and external pores are present, the deformation is preferential towards the larger external pores.

7. Acknowledgements

The authors would like to thank the National Metal and Materials Technology Center, Thailand for research grant MT-B-46-MET-07-131-NI. The valuable discussions with our colleagues at Particulate Materials Program are also very much appreciated.

8. References

[1] Bolarin, A. M., Sanchez, F., Barba, A., Coreno, O. and Coreno, J., "Electroless nickel plating of atomised and sponge tron compacts", Surface Engineering, Vol. 19, No. 5, 2003, pp. 364-368.

[2] Liu, Y., German, R. M. and Engel, R. S., "Finite element modeling for loose powder compaction", Proceedings of the World Congress on Powder Metallurgy and Particulate Materials, 30 May-3 June 2000, New York, NY, USA.

[3] Wu, W., Jiang, R. H., Wagoner, R. H. and Daehn, G. S., "Experimental and numerical investigation of idealized consolidation–Part 1: static compaction", Acta Materialia, Vol.48, 2000, pp. 4323-4330.

[4] Gethin, D. T., Ransing, R.S., Lewis, R.W., Dutko, M. and Crook, A. J. L., "Numerical comparison of a deformable discrete element model and an equivalent continuum analysis for the compaction of ductile porous material", Computers & Structures, Vol. 79, 2001, pp. 1287-1294.

[5] Mori, K. and Kuzime, R. "Microscopic approach of powder compaction using finite element method", International Journal of Mechanical Sciences, Vol. 44, 2002, pp. 793-807.

[6] Tanwongwan, W., Otarawanna , S., Manonukul, A., and Carmai, J., "Effects of circular and elliptical particles on metal powder compaction process", Proceedings of First Metal Forming Conference 2004, Bangkok, Thailand.

[7] Tanwongwan, W., Manonukul, A., and Carmai, J., "Effects of powder size and initial arrangement on cold compaction", JSME/ASME International Conference on Materials and Processing 2005 (M&P 2005), Seattle, WA, USA, 19-22 June 2005.

[8] ABAQUS Theory Manual, Version 6.3, Hibbit, Karlsson and Sorenson, RI, 2002.

[9] www.hoeganaes.com [2005, September 8]

[10] Gurson, A. L., "Continuum theory of ductile rupture by void nucleation and growth–Part 1: yield criteria and flow rules for porous ductile media", Journal of Engineering Materials and Technology, Vol. 99, 1977, pp. 2–15.

[11] ABAQUS Explicit Manual, Version 6.3, Hibbit, Karlsson and Sorenson, RI, 2002.

[12] http://www.hoganas.com/pages/cgi-bin/PUB_Latest_ Version.exe?pageId=5&allFrameset=1 [2005, September 8]

Appendixes

Appendix A Calculation of apparent density in two-dimensional

The density of Ancor® MH-100 is 2.55 g/cm^3.

The density of solid wrought iron is about 7.568 g/cm^3.

$\therefore$ The relative density of Ancor® MH-100 is

$$\frac{2.55}{7.568} \approx 0.333.$$

The relative density of HCP unit cell in 2D is 0.907 whilst that in 3D is 0.74.

$\therefore$ The relative density of Ancor® MH-100 in 2D is $0.333 \times \frac{0.907}{0.74} \approx 0.4$.

Appendix B Calculation of apparent density of each sponge powder

The relative density of HCP unit cell in 2D is 0.907.

The relative density of Ancor® MH-100 in 2D is 0.4.

$\therefore$ The relative density of each Ancor® MH-100 powder in 2D is $\frac{0.4}{0.907} = 0.44$.

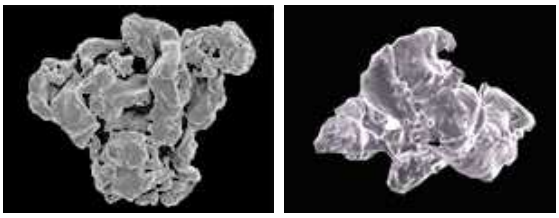

(a) sponge powder (b) solid powder

Figure 1 SEM photomicrographs of (a) sponge powder and (b) solid powder fabricated from oxide reduction and atomisation respectively. [12]

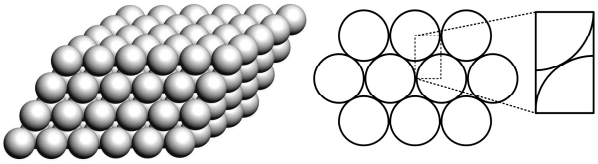

(a) 3D (b) 2D and its unit cell

Figure 2 Hexagonal-closed-packed arrangement of mono-size circular particles and the corresponding representative unit cell.

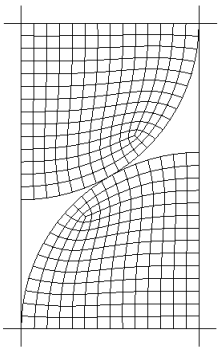

(a) solid powders and sponge powders defined by the constitutive modelling .

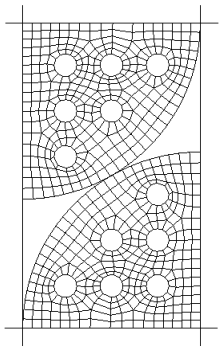

(b) sponge powders using the 'explicit modelling of internal pores' approach.

Figure 3 Finite element models for uniaxial compactions of solid and sponge powders.

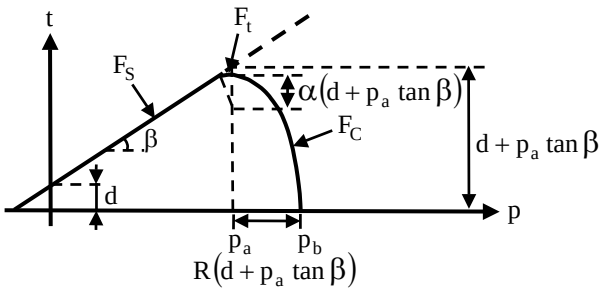

(a) modified Drucker-Prager Cap model

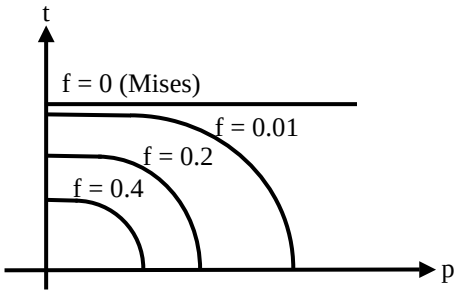

(b) porous metal plasticity model

Figure 4 Yield surfaces of (a) the modified Drucker-Prager Cap model and (b) the porous metal plasticity (Gurson) model.

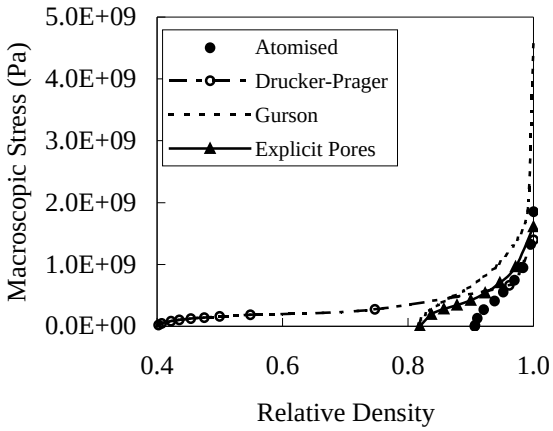

Figure 5 Macroscopic stress responses of the solid and sponge powder compactions at different relative densities.

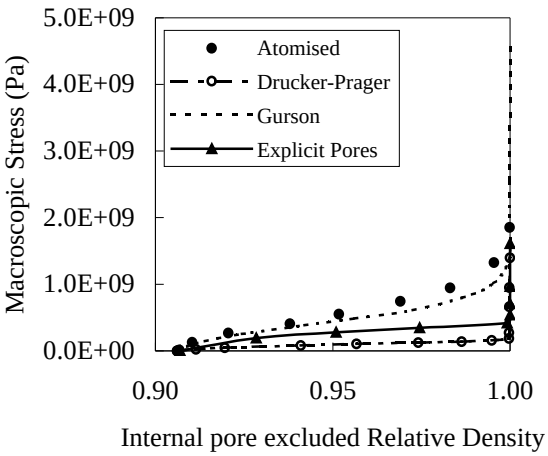

Figure 6 Macroscopic stress responses of the solid and sponge powder compactions at different relative densities excluding internal pores.

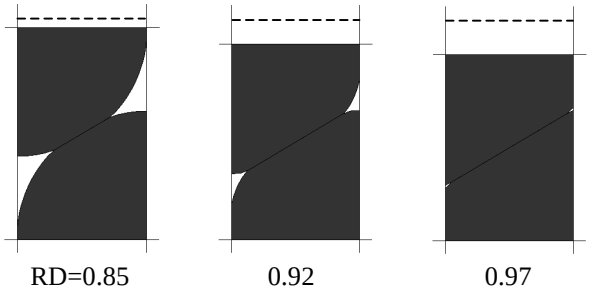

(a) the porous metal plasticity (Gurson) model

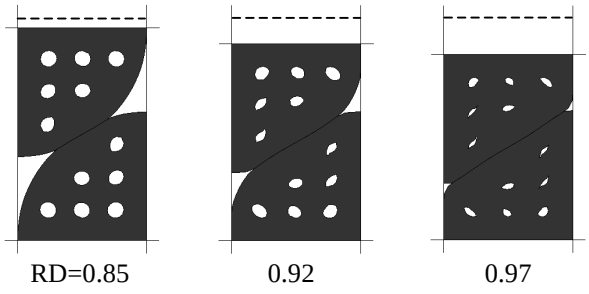

(b) 'explicit modelling of internal pores' approach

Figure 7 The deformation shapes of the sponge powder (a) defined by the porous metal plasticity (Gurson) model and (b) using 'explicit modelling of internal pores' approach at different relative densities shown.

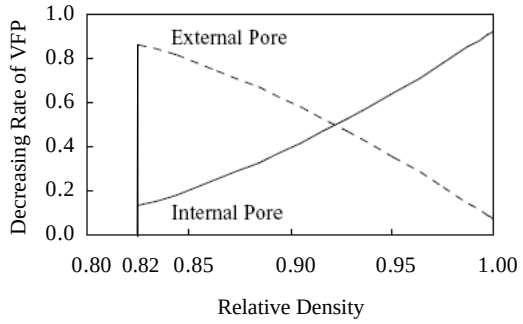

(a) the porous metal plasticity (Gurson) model

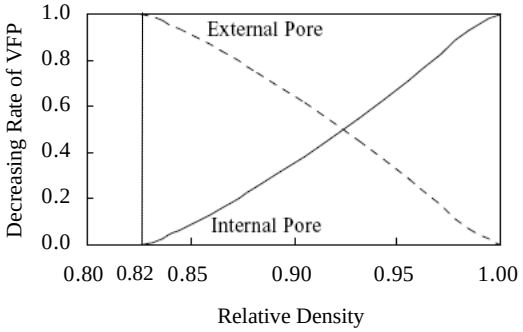

(b) 'explicit modelling of internal pores' approach

Figure 8 The decreasing rate of change of the volume fraction of internal or external pores with respect to the rate of change of the total volume fraction of pores for the sponge powders (a) defined by the porous metal plasticity (Gurson) model and (b) using 'explicit modelling of internal pores'.